POLITECNICO DI TORINO
Repository ISTITUZIONALE

Optimization of Three-Dimensional (3D) Multi-Sensor Models For Damage Assessment in Emergency Context: Rapid Mapping Experiences in the 2016 Italian Earthquake

Publisher copyright

(Article begins on next page)

04 August 2020

Optimization of Three-Dimensional (3D) Multi-Sensor Models For Damage Assessment in Emergency Context: Rapid Mapping Experiences in the 2016 Italian Earthquake

Giulia Sammartano

Politecnico di Torino, Department of Architecture and Design, Torino, Italy;
giulia.sammartano@polito.it

Abstract: Geomatics techniques offer the chance to manage very cost-effective solutions for three-dimensional (3D) modelling, from both the aerial and terrestrial point of view, with the help of range and image-based sensors. 3D spatial data that is based on integrated documentation techniques, featured by a very high-scale and an accurate metric and radiometric information nowadays are proposed here as metric databases that are applicable for assisting the operative fieldwork in the case of rapid mapping strategies. In sudden emergency contexts for damage and risk assessment, the structural consolidation and the security measures operations meet the problem of the danger and accessibility constraints of areas, for the operators, as well as to the tight deadlines needs in first aid. The use of Unmanned Aerial Vehicles (UAVs) equipped with cameras are more and more involved in aerial survey and reconnaissance missions; at the same time, the ZEB1 portable Light Detection and Ranging (LiDAR) mapping solution implemented in handle tools helped by Simultaneous Localization And Mapping (SLAM) algorithms can help for a quick preliminary survey. Both of these approaches that are presented here in the critical context of a post-seismic event, which is Pescara del Tronto (AP), deeply affected by the 2016-2017 earthquake in Central Italy. The Geomatics research group and the Disaster Recovery team (DIRECT—http://areeweb.polito.it/direct/) is working in collaboration with the Remotely Piloted Aircraft Systems (RPAS) group of the Italian Firefighter.

Keywords: emergency UAV mapping; SLAM; cultural heritage risk; multi-sensor documentation; multi-scale modelling

1. Introduction

Currently, the contribution of the latest Geomatics research in the field of rapid mapping strategies offers the chance to manage very cost-effective solutions for three-dimensional (3D) metric and radiometric documentation, with very high-scale from both the aerial and the terrestrial point of view. The recently implemented approaches in the Geomatics research, together with the commonly explored ones, can be developed for an effective and operative fieldwork, especially in sudden emergency contexts for damage and risk assessment, security measures, and structural consolidation intervention. In fact, in most of the urban centers where the built heritage retrieves the demand of damage documentation and data management and sharing as efficiently as possible, are now encountering the problem of the danger limitation and accessibility constraints of the areas for the operators as well as to the tight deadlines needs in first aid. The solutions to be investigated seem increasingly to be the ones that allow for rapid mapping using both image-based and range-based approaches.

Imagery methods based on sets of collected images following photogrammetric methods that can now rely on the exploitation of image matching and Structure from Motion (SfM) algorithms, which are derived from the computer vision field, can be considered nowadays as a quick means for a low-cost mapping and 3D reconstruction.

The use of Unmanned Aerial Vehicles UAVs equipped with cameras are more and more involved in aerial survey and reconnaissance missions, and they are behaving in a very cost-effective way in the direction of 3D documentation and preliminary damage assessment. More and more UAV equipment with low-cost sensors must become, in the future, suitable in every situation of documentation, but above all, in damages and uncertainty frameworks. Rapidity in acquisition times and low-cost sensors are challenging marks, and they could be taken into consideration maybe with time spending processing.

Even range-based methods based on Light Detection and Ranging (LiDAR) scans are an increasingly used solution but considering the time needed for recording, registering, filtering, and decimation of points clouds, as well as the construction of the 3D mesh, the Terrestrial Laser Scanning (TLS) technique is used when strictly necessary. TLS provides extremely detailed and accurate outputs, but is definitely heavy and less sustainable in relation to photogrammetry. Some mobile scanning solutions are being recently developed for indoor/outdoor environment mapping. These portable systems are based on Simultaneous Localization And Mapping (SLAM) technology and allow for quickly collecting a big amount of 3D metric data, in the form of point cloud, not only for the building scale, but also for surrounding context objects in an environmental documentation scale.

This paper wants to base its proposal on the possibility of analysis, interpretation, and classification of metric and non-metric withdrawable information, starting from 3D aerial and terrestrial high-scale models. These attained starting metric data offer the possibility to carry out a global assessment on them and on their ability to reach a level of detail and consequently meet the most suitable scale. After their metric accuracy control, it should be possible to use these 3D models and their geometries as suitable for further uses as the structural analysis one.

This process is planned in the direction of quick surveys and targeted operation helpful to assess the state of conservation and seismic damage in these types of building belonging to a precarious context. The selection of survey methods depends primarily on these issues, and then it is influenced by the needs of information detection on those models. Metric data and its extraction constitutes the unavoidable base on which to base non-metric information, as visual and qualitative ones. The aim of this research is to evaluate the contribution of terrestrial and aerial quick documentation based on image-based and range-based techniques for quick 3D modelling, gathered specifically here by a SLAM based portable LiDAR and a multirotor UAV equipped by camera, for a first reconnaissance inspection and modelling in terms of level of details, metric, and non-metric information.

The test case is an experience of Cultural Heritage documentation specifically in disaster areas in the center of Italy, carried out by Politecnico di Torino from August 2016 up to now. In these areas, a strong earthquake occurred in August 2016, and current ongoing seismic shocks still take place. The moment magnitude of this event is listed as 6.0 by INGV (Istituto Nazionale di Geofisica e Vulcanologia, http://cnt.rm.ingv.it/), which places the hypocenter depth of the event at 8 km. Two earthquakes occurred after the first event in 24 August: an event on 26 October, with a 5.9 moment magnitude, and another one (the largest event) on 30 October with a 6.5 moment magnitude. In this scenario, quick surveys, damage assessment, and diffuse and urgent measures of safety and consolidation were required. This study is carried out specifically on some selected buildings in Pescara del Tronto (Ascoli Piceno), where a multi-sensor 3D survey was performed in repeated missions in September, October, December, and February.

2. Multi-Sensor Documentation in Emergency Areas

2.1. Methodological Framework

In recent years, we can affirm that the increasing use of Remoted Piloted Aircraft System (RPAS) equipped with cameras have already improved its role in competitiveness and efficiency in surveying operation on the field. The

phenomenon is nowadays covering many application domains (e.g., geomatics, geotechnics, archaeology, forestry, structural analysis, etc.). The current aspect is also connected to the diffusion of a large number of operators (not expert people as well) and concurrently to the efficient image-matching algorithm based of SfM photogrammetry even more suitable for 3D information extraction from images and frames videos that are acquired by compact cameras that are embedded in low cost commercial drones. The use of drones equipped with cameras and/or high-definition video devices, along with on-board GPS systems, have thus grown in its recognized role for aerial documentation finalized to metric survey purposes. It is moving in a very profitable way in many contexts due to low-cost and non-hazardous characteristics, and, as is well known in recent research experiences, is very popular for the 3D documentation and monitoring Cultural Heritage sites (Chiabrando et al., 2016a; Ruiz Sabina et al., 2015; Lerma et al., 2012; Remondino et al., 2011).

In particular, photogrammetry by drones is proving increasingly crucial in emergency situations, not only for remote observation of sites and emergency action planning for the collection of qualitative information, but also for production of very large scale metric data (Boccardo et al., 2015; Wang et al., 2013; Hirokawa et al., 2007).

During the last ten years, the use of drones became equally diffuse in urban areas involved in natural disaster for preliminary search and rescue, Building Damage Assessment (BDA) (Meier, 2016; Fernandez et al., 2015). This is sometimes preferred more than the more traditional vertical images from remote sensing data. Due to their scale, their geometric configuration, and ultimately their intrinsic features, satellite imaging does not satisfy the requirements of details and information (Lemonie et al., 2013; Rastiveis et al., 2013; Gerke and Kerle, 2011).

The first data acquisition phase, to be done as quickly as possible after a disaster, is ordinarily carried out in person with many efforts by technicians in damaged sites, and it is a heavy time-consuming operation. Rapidity in acquisition times must be effectively balanced with post processing times, as well as the time-cost ratio must be successful, in favour of low-cost sensors with their top efficiency, as the best possible compromise between timeliness and accuracy (Lemonie et al., 2013). It must maximize, ultimately, the density of data and the metric data extraction from 3D models that are processed ex post, without neglecting productivity in ex ante data acquisition in emergency circumstances, where the practicability of spaces that are connected to the high risk they could cause, can adversely affect the quality of data. Moreover, 3D models already are, and could be increasingly in the near future, an essential platform of dense information for interdisciplinary teamwork on the object of study, which will be analysed in remote, in a second step, for many purposes. They could be, for example: emergency measures of rescue and second aid for civil protection and firefighters,

or for damage detection and structural assessment, and for planning a structural strengthening project, or even historical documentation studies, as well as restoration analysis and intervention.

2.2. Regulations on Damage Assessment via Documentation Techniques

A 3D survey for damage sites needs some important considerations in terms of time-costs, as well as human involvement, on balancing the acquisition phase resources and the processing ones. Traditional survey techniques have restrictions in different issues. Ground-based mapping is complex, sometimes dangerous for expert operators and data acquisition is largely limited to terrestrial point of view and façade information. On the other hand, medium range image-based mapping is typically restricted to vertical views for the roof condition, but for collapses, lower levels of damage are much harder to map, because such damage effects are largely expressed along the façades, which are not visible in such imagery (Gerke and Kerle, 2011).

Most operational post-disaster damage mapping, such as the processing of satellite data, acquired through the International Charter "*Space and Major Disasters*" (https://www.disasterscharter.org), remains based on visual interpretation (Voigt et al., 2011; Kerle, 2010). Anyway, also high-resolution satellite images, due to their scale, their geometric configuration, and ultimately their intrinsic features, do not respond comprehensively to the demand of details and information for the scale and complexity of urban context to a clear identification of the damage (Lemonie et al., 2013; Rastiveis et al., 2013; Gerke and Kerle, 2011). Multi perspective oblique imagery, as it is known in literature, seems to be the profitable solution to maximize detail on buildings. For the 3D data processing, many ways can be followed: from a merely visual one for qualitative information, to a manual one, managed by operator on points clouds and 3D models, up to an automatic data extraction. Automatic image analysis techniques for BDA can be broadly grouped into pixel and object-based methods (Fernandez et al., 2015).

For damage assessment, we have thus to chase the solution of integration and/or fusion of nadir oblique cameras where possible, integrated by terrestrial information only if necessary. These multi-sensors models are a kind of complex informative database that must approaching to be a final-use based model: metric and non-metric information define the geometric and conservative characterization. For example, the structural analysis and damage assessment on masonries, in this case, for post-earthquake contexts, establishes the setting up of damage scenarios on the preliminary interpretation and evaluation of visible damages features on the objects. The classification on EMS-98 scale (European Macroseismic Scale) of damage is based on building types. Particularly, for each type of masonry structure, depending on the employed materials and constructive

techniques, an empiric vulnerability class is associated (descending scale from A to E) and a level of damages is categorized observing the structure (from 1 to 5) (Figure 1).

Figure 1. Classification of damage to masonry buildings from EMS-98 scale (European Macroseismic Scale) (Grunthal, 1998).
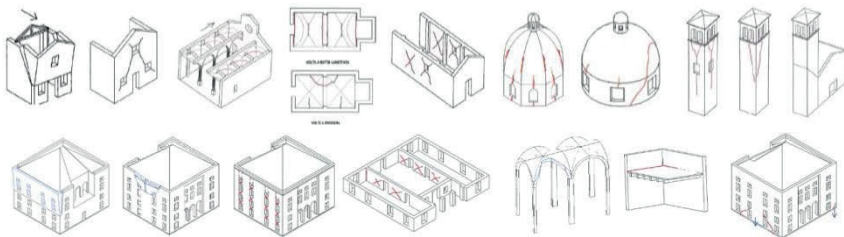

Figure 2. Excerpts from "Abacus of collapse mechanisms" in case of damages assessment of Cultural Heritage, datasheet A-DC "Churches" and B-DP "Buildings" (DPCM 23/02/2006).

The Italian regulation takes into account through several updated regulations over the years the survey finalized to the damage mapping and indexing in a standardized format. The *AeDES* datasheet *(C.N.R.-G.N.D.T. and S.S.N. in Department of Civil Protection),* is the 1st Level datasheet and has been organized in order to help the damage detection and assessment, emergency response, and practicability, for ordinary buildings in post-earthquake emergence. More specifically, it can be possible to approach to monumental buildings with the datasheet for the damage regarding palaces B - DP (2006) and churches A - DC (2011). According to the Ministerial datasheet A-DC and B-DP, the ability to define the structural behavior of the masonries building with its elements is described in the Figure 2 for "Churches" and "Buildings". The potential of metric and non-metric information enclosed in high-definition 3D point clouds and models completed by quick mapping is useful to reach this type of level of detail, and potentialities are many and very remarkable in relation to the classification of potentially recognizable damage to a first visual analysis of artefacts.

3. Testing Rapid Mapping in Pescara Del Tronto after 2016 Earthquake

After the earthquake occurred in August 2016 in the center of Italy, DIRECT Team (Disaster Recovery Team) from Politecnico di Torino in cooperation with the

GEER team (Geotechnical Extreme Events Reconnaissance Association), and with the Remotely Piloted Aircraft Systems (RPAS) group of the Italian Firefighters were involved in several reconnaissance and metric survey missions. In September, October, November 2016, and February 2017, the goals were the rapid mapping of villages and a focused multi-sensors documentation of buildings in urban areas that were deeply repeatedly damaged by shocks. Numerous villages had been involved, such as Pescia, Pescara del Tronto, Cittareale, Accumoli, Norcia, Castelluccio, Amatrice, etc.

The present contribution is focused on the ancient perched village of Pescara del Tronto (Figure 3), in Arquata del Tronto municipality. The techniques that were deployed by the teams have been focused on the documentation post-disaster of the whole village with multi-scale approach and resulting assorted multi-sensor acquisitions. Groups of differently damaged buildings were examined, with the combined use of terrestrial and aerial sensors.

Then, a test area was chosen in the northern part in the specific focus of a stand-alone damaged building, an integrated metric survey has been conducted and was tested in order to evaluate both multi-sensor model information and processing resources. Moreover, after a subsequent earthquake event occurred in the end of October and with the contribution of the mission in December a new 3D model post-event has been available.

Figure 3. Pescara del Tronto in Arquata del Tronto municipality (Ascoli Piceno), is one of the perched villages allocated across the Apennines mountain in Marche region (left, center), center Italy, on the border with regions Abruzzo, Lazio, Umbria. It was destroyed by the reiterated seismic shocks from

It is important to underline that, due to the sequence of earthquakes, the access at many damage sites of interest remains difficult because the sites were (and still are) located in restricted red zones, and are dangerous because many of the structures are unstable and are still prone to collapse. Notwithstanding the site challenges that have made us think about sensor choice and acquisition planning, the higher part of Pescara del Tronto village was accessible. Terrestrial LiDAR technique was excluded regardless, due to the emergency purposes of the mission in those sites. Therefore, for these problematic sites, the preferred approach to

investigate their damage involved the use of photogrammetric-based acquisition using UAV, which were integrated with traditional close-range acquisition systems wherever feasible. Next to these ones, a quick SLAM based LiDAR scan was tested.

First of all, in order to define a common reference system for the RPAS and terrestrial acquisition, Global Navigation Satellite System (GNSS) and total station measurements were performed. As Ground Control Points (GCPs), several markers were placed on the area and were then measured using the GNSS in Real Time Kinematic (RTK) mode (Figure 4). Together with the GNSS measurements, some natural points using a total station side shot approach were measured on the façades of the damaged buildings in order to be used during the photogrammetric process. The measured points were georeferenced in a common reference system (UTM-WGS 84 Fuse 33 N ETRF 2000) using the information derived from the Italian Dynamic permanent network controlled by the Italian Geographic Military Institute (IGM, http://www.igmi.org/).

The whole area in Pescara del Tronto involved in the metric survey was covered by almost 40 GCP materialized on ground by targets as Figure 4. Three of these targets where positioned in the neighborhood of the damaged building. Moreover, for each building that was measured and imaged by multi-sensor acquisitions, a set of natural points were detected on buildings. For the buildings blocks points have been measured on the main elements, as the roof edges, the façade, the windows and the door, and the stone elements are useful for both the aerial and the close-range blocks.

Figure 4. Survey operation during the setting up of the topographic measurements. A moment of the aerial markers planning and placing on ground with fire fighters (left). Global Navigation Satellite System (GNSS) measurements on target disseminated in more or less accessible areas in the neighborhood of the damaged building, with the Leica System 1200 GNSS receiver (center left and right), Leica TS06 total station topographic survey (right).

3.1. UAV Platforms for High-Scale Aerial Documentation

The teams incorporated multiple aerial platforms and image-based sensors including COTS (commercial off the shelf) platforms and a customized professional UAV fixed-wing platform (Figure 5). The acquisition strategy for each system varied based on its strengths and capabilities, but provided a wide range of

remote sensing data that can be used for subsequent focused processing and analysis. The aim is to test them in different scenarios and setting acquisitions to evaluate their contribution of aerial imaging, by nadir and oblique points of view, in the 3D definition of the building geometry, in terms of details and metric/radiometric information to be extracted too (Chiabrando et al., 2017). Moreover, a georeferencing strategy for the ZEB mobile mapping system point clouds is proposed. It is based on the geometrical features provided by the high-scale aerial point clouds.
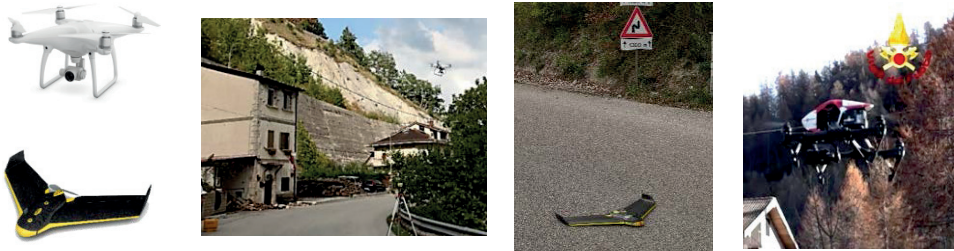

Figure 5. The fleet of aircrafts used in Pescara del Tronto by the Disaster Recovery Team (DIRECT) Team in cooperation with Firefighters Remotely Piloted Aircraft Systems (RPAS) corp. The Phantom 4 DJI (top left) flying (third from right image), the Ebee by Sensfly (down left) at the take-off phase (second from right); the customized Inspire 1 by DJI, property of Firefighters (first from right).

3.1.1. A Fixed Wing UAV: eBee by Sensfly

The first flight over the settlement of Pescara del Tronto was performed with an eBee™ small UAV platform, manufactured by Sensefly and commercialized in Italy by Menci Software (http://www.menci.com) (Figure 5). In this case, the UAV was equipped with a digital camera Canon Power Shot S110™, which offers a 1/1.7" Canon CMOS sensor, 12 MP images, and a focal length of 5.2 mm. The platform is extremely manageable and very useful for rapid map realization in emergency (Boccardo et al., 2015). The eBee system is certified by ENAC as EBM-1539 and it is approved as inoffensive. In order to cover all the damaged areas (almost 83 ha) three flight with the following characteristics were realized: mean flight height 150 m; expected Ground Sample Distance - GSD= 0.05m; Side overlap 60%; Forward overlap 85%.

3.1.2. Multirotor Aircrafts: Phantom 4 and Inspire 1 by DJI

The other flights over Pescara del Tronto were performed using multirotor aircrafts that were deployed for a closer acquisition on focused buildings blocks (Figure 5).

A Phantom 4™ quadrotor small UAV, manufactured by DJI (*Dà-Jiāng Innovations Science and Technology Co., Ltd Technologies*) has been used. The Phantom 4 is equipped with a 4K video camera that has a 1/2.3" CMOS sensor, 94-degree field of view, 12.4 MP images, and a focal length of 20mm. The Phantom 4 system weighs 1.38 kg, has a maximum flight time of 28 min, and offer the ability to hover and/or collect imagery from vertical faces. Those flights were performed manually with an experienced UAV operator. Imagery from the UAV was transmitted to the operator in real time, ensuring significant image overlap, while maneuvering the UAV to capture the skewed imagery from objects of interest. This approach was also used successfully following the 2014 Iquique earthquake (Franke et al., 2016). The flight with the DJI was performed at an elevation ranging from 10 m to 20m. The data were acquired by UAV (Figure 7), specifically, following the two available approaches: the 4K video recording (and then the frame extraction) and the single shooting set-up, that allow for acquiring nadir and oblique images and videos. A set of 64 nadir images were acquired by DJI camera; moreover, almost 140 frames were extracted from the 08:19 min video with 29 frames/sec (1frame/3.5sec).

Furthermore, a quadcopter INSPIRE1 by DJI, customized by the SAPR team of Italian Firefighters group was used. The weight of about 3kg with (maximum weight at take-off 3.5 kg) and an extreme adaptability, manually piloted or with planned flight, offers a flight range of 20 minutes. It is equipped by the Camera ZENMUSE X5, CMOS sensor, focal length 15mm F/1.7-F/16, field of view 72°, for 4K video and images 16 MP (4608x3456), and offers oblique and nadir images acquisition.

3.2. Hand-Held Mobile Mapping Scanner: ZEB1 by GeoSLAM

In a post-disaster scecatnario and with the need to evaluate the contribution of different methods for the documentation of the damage, a 3D mobile mapping system (Figure 8) was tested. Among the available alternatives, we opted for the hand-held Zeb1 system by Geoslam (http://geoslam.com/).

This device (Figure 8) consists in a two-dimensional (2D) lightweight time-of-flight scanner with 30 m outdoor maximum range (*Hokuyo scanner*) and an Inertial Measurement Unit (IMU), which roughly ensure the altitude. They are both mounted on a spring so that when the operator moves in the environment to be mapped, the device swings freely and randomly determining the 2D scanning plane invests the environment generating a 3D point cloud (Bosse et al, 2012). The

mapping system is based on the SLAM technology, which is the mostly suitable for indoor environments since it uses the environment geometric features to update the position of the device (Riisgaard and Blas, 2005). ZEB1 uses the raw trajectory to roughly calculate the surface normals and potential constraints (features recognition) within a single sweep of the scanner. Then, a *cloud-to-cloud* registration of the point cloud profiles generate the 3D cloud using an iterative process, which relies on geometric objects and features within the scans. The importance of the features constrains, essential to align subsequent scans, is visible in Figure 8, which shows how the quality of the recording is less accurate when the operator has moved away from the building. Although the system is provided for outdoor/indoor mapping, the processing presented in the next paragraphs show different accuracies and the level of detail for different portions of mapped objects, as other tests performed (Thomson et al., 2013). The consideration that the cloud was acquired in few minutes shows the remarkable interest of this system.
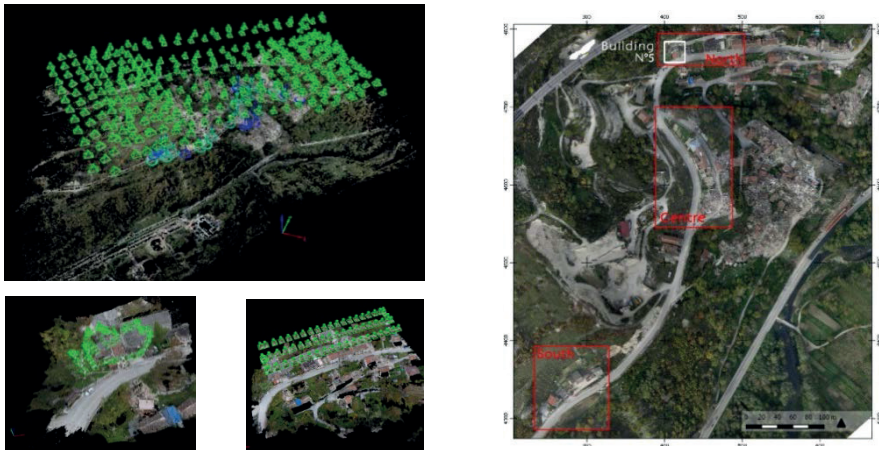

Figure 6. The eBee flight on Pescara del Tronto, organized in three grid blocks: the bigger longitudinal one on the village, and two lateral ones, perpendicular to the mail grid (top left). (down left) An example of oblique (left) and nadir grid (right) acquisition by multirotor DJI. The three test areas are pointed out on the eBee aerial orthoimage, GSD of 5 cm (right), in which the integrated survey by ZEB1 scans and UAV photogrammetry was performed and focused on building n°5 (white square).

Figure 7. Samples datasets of acquired images by flights. North area, Phantom4 (first row) and South area, Inspire1 (second row).

3.3. Point Clouds Data Processing and Integration for Rapid Mapping in Three Test Areas

In order to test a rapid mapping method in this critical area, three areas that were characterized by different geometric conformation characteristics have been chosen (Figure 6). Meanwhile, a post disaster damages survey and assessment, together with structural analysis, were developed by experts.

Due to the extremely difficulty of the site, the topographic and GNSS survey had to be flexible and rapid. Single alone Total Station vertices were set for the detail measurements on spot buildings all over the village of Pescara del Tronto; it were located on aerial targets placed on the surrounding, and measured using the GNSS in RTK mode. So, the whole data processing is directly affected by the precision of the topographic measurements, bound by the precarious area.

For the first processing step each data collection from different sensors were processed in separate blocks:

− *Terrestrial close-range photogrammetry performed walking around the buildings blocks*
− *Fix wing UAV nadir cameras (150 m altitude) generate a 3D photogrammetric model of the whole city.*
− *Multirotor nadir and oblique cameras (variable altitude) focused on the buildings blocks*
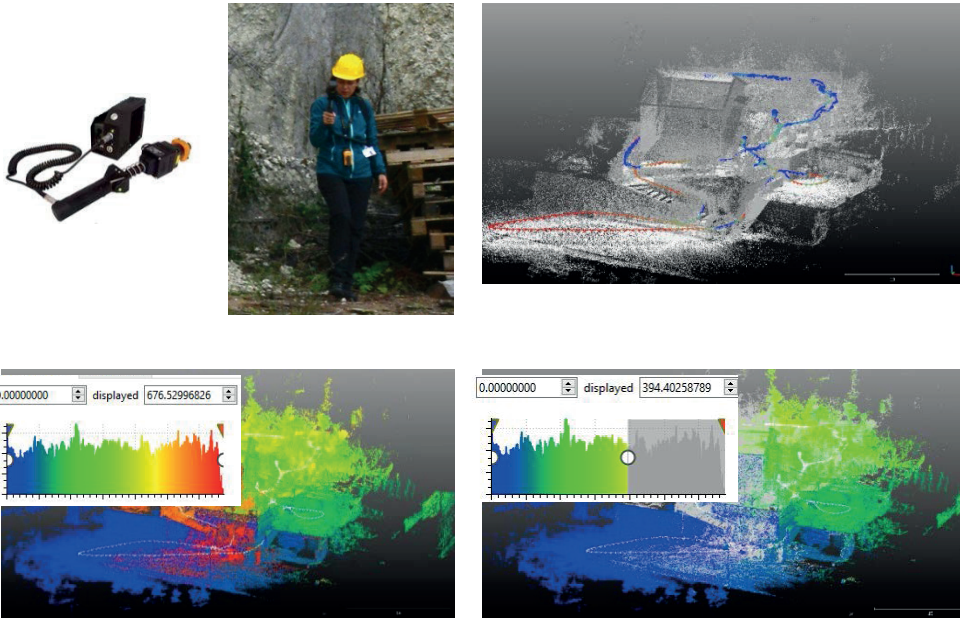− *ZEB1 survey around buildings and blocks.*

152

Figure 8. (Top left) The portable ZEB1 system and the operator during an acquisition. (Top right) The raw b/w point cloud and its path, in scalar colour to indicate the quality of registration. (Down left) The point cloud visualization in scalar colour according to "time" variable (seconds unit); in white colour the path. (Down right) A selected portion of point cloud at the beginning of the acquisition: the first six minutes.

For the processing of the photogrammetric blocks three commercial software were tested, with different dense image - matching algorithms: Pix4D (https://pix4d.com) by EPFL Innovation Park, workflow is based on a Structure From Motion approach (Strecha, 2014); Context Capture by Bentley System (https://www.bentley.com), Photoscan Pro by Agisoft (http://www.agisoft.com). For point cloud treatment, optimization, 3D modelling and analysis 3DReshaper (http://www.3dreshaper.com/) by Tecnodigit-Hexagon and open source Cloud Compare (http://www.danielgm.net/cc) were employed. A workstation with high performance hardware was exploited: CPU: Intel(R) Core i7-6800k 3.4 GHz. RAM 128 GB. NVIDIA quadro M2000.

3.3.1. Aerial Photogrammetry Point Clouds

The aerial acquisition, which was performed with different aircrafts, covered two main detail requirements and, as a consequence, two different scales, as it is pinpointed in Table 1. *eBee* complete cameras block was processed to produce a 3D model as an overview of the village in its environment according to a landscape

scale (Figure 6). Time of processing of almost three hours provided a high quality point cloud, 3D model, and DSM (15Gb data), as we can see in Table 1, with GSD is almost 5cm. Aerial images, originating by multirotor UAV, from both acquisition by cameras positions and frames extracted from HQ video, have been oriented with GCPs, and the achieved models (almost 10 hours) offer an accuracy of a mean value of 0.095 m on Ground Control Points (GCPs) and an average value of 0.025 m on Check Points (CP)s.
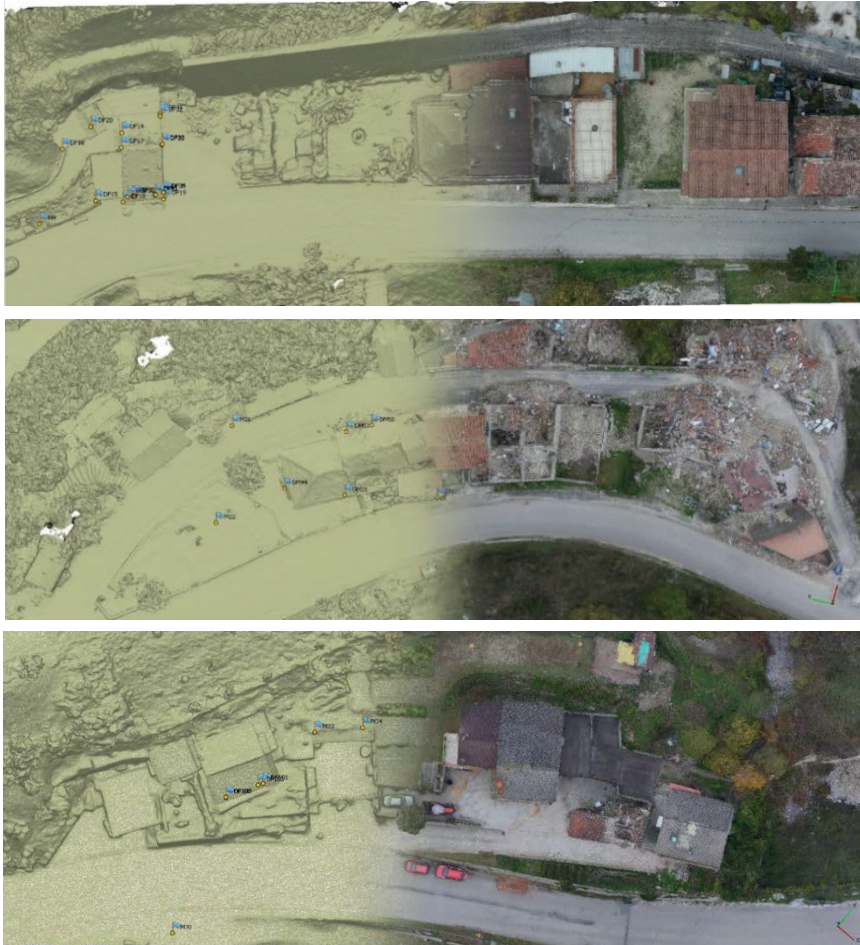

Figure 9. The polygonal surface model of the dense point cloud generated with Photoscan workflow from the UAV images, without and with RGB information. (From the top) the Northern, the Central, the Southern blocks.

High scale aerial models, with a mean GSD of 1.3 cm/pixel, have been calculated (Figures 6 and 9):

- *NORTHERN AREA* (*Buildings n°5 and n°6*), a moderately flat area with stand-alone buildings facing the street. A huge rock wall stands behind the buildings block, on which the viaduct is set.
- *CENTRAL BLOCK* (*n°4*), a big block bounded between two semi-parallel streets connecting north and south village areas with a difference in height of about 2m.
- *SOUTHERN AREA* (*Buildings n° 1, n° 2 and n° 3*), a significantly complex context, with a group of buildings arrayed on a difference in height of about 7 m. Behind a very impassable space with thick vegetation.

Table 1. Synthesis table of aerial datasets, processing, Root Mean Square Error (RMSE) on Ground Control Points and Check Points.

	Data Processing Results about Aerial Photogrammetric Blocks		
	EBEE	**PHANTOM 4 DJI**	**INSPIRE 1 DJI**	
		North	*Center*	*South*
Camera config.	nadir	nadir+oblique	nadir+oblique	nadir+oblique
Area Covered (m²)	830,000	6,390	17,100	13,100
Flight altitude (m)	150	35	95	55
Cameras n°	354	380	256	291
Image resolution	3000x4000			
av. GSD (cm/px)	5	1.11	1.65	1.18
tie points	1,505,299	264,452	402,924	313,981
Dense point cloud	104,733,709	27,802,455	28,853,157	21,219,411
RMSE on GCPs(m)	**0.026**	**0.0198**	**0.0194**	**0.0202**
X	0.022	0.0227	0.0208	0.0196
Y	0.024	0.0151	0.0136	0.0174
Z	0.032	0.0216	0.0237	0.0235
RMSE on CPs (m)	**0.036**	**0.0428**	**0.0174**	**0.0190**
X	0.031	0.0248	0.0215	0.0164
Y	0.016	0.0135	0.0062	0.0100
Z	0.058	0.0903	0.0245	0.0306

3.3.2. ZEB1 Point Clouds

In Pescara del Tronto, ZEB1 instrument was tested in many areas with groups of buildings, with different configurations in the acquisition trajectory. In these test areas, different point clouds (Table 2) were processed by automatic SLAM Cloud-to-cloud registration in GeoSLAM *pay-as-you-go* cloud processing. The crucial point of this technology is the control of the trajectory during the movement, which is estimated and corrected because of the 3D cloud that was acquired using a variation of traditional ICP (iterative closest point) scan-matching (Bosse et al., 2009). The development of the system has taken advantage of the opportunity to help the correction by the execution of closed loop trajectories during the mapping path, which also leads to better assess to the overall quality of the final 3D cloud.

The marketed system guarantees an absolute accuracy of position variable between 3 and 40 cm depending on the type of environment that is mapped (http://geoslam.com/).
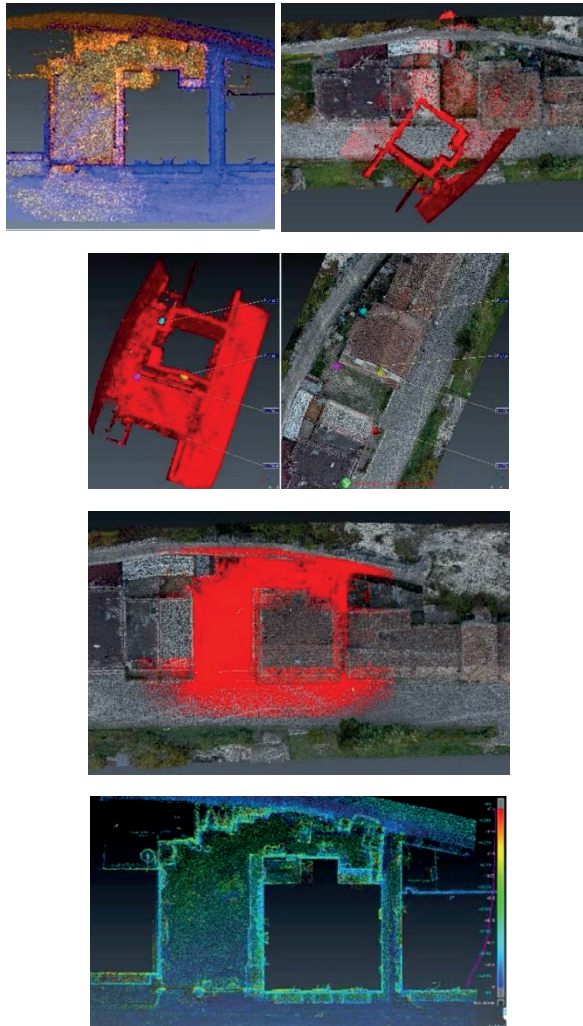

Figure 10. The process of registration and georeferencing of the ZEB point cloud through the fitting algorithms with the aerial point cloud. The co-registration of two ZEB clouds (orange, blue) around a building and its courtyard in Northern area (top, left). The cloud union (red) not georeferenced (right). The preliminary alignment with corresponding points coordinates (down, left) and the georeferenced result after *cloud-to-cloud* fitting (right).

In Pescara del Tronto, due to the critical area conformation and the contingent performance of the path, the procedure of cloud registration ended with a residual error of up to 30 cm. Another advantage of the system is that the results are offered as a series of structured datasets, relative to the cloud and the trajectory, offering the ability to segment the cloud using the time function (Figure 8). After a point cloud processing according to the time (time data embedded in the 3D data), alignment with other ZEB clouds (Figure 10), segmentation, post registration, georeferencing, and optimization, the point cloud was ready to be analyzed with other sensors results, with the lack of radiometric information.

Due to the experimental use of these clouds, some problems about point clouds SLAM registration related to context complexity occurred. Different processing strategies are preliminary proposed in order to georeference and empirically improve the alignment of row ZEB1 points characterized by acquisition time:

- Georeferencing ZEB cloud attributing coordinates on identifiable homologous points,
- Georeferencing ZEB cloud with points and optimizing with fitting algorithms on *aerial point cloud*, and
- Segmentation and georeferencing ZEB cloud if any there would be errors during the acquired trajectory and bad quality clouds registration; then, optimization with fitting algorithms on the aerial point cloud.

According to these first experimental tests (Table 2), the *Central area*, in which a closed semi-circular path was performed, without retracing in the return the outbound track, reports the worst results. The need of quite close geometrical features around which the scan sustains the SLAM processing of progressive registration is thus very crucial. Changes of elevation with extensive spaces in these complex contexts have proven to be no help for a recording with a controlled error lower than 10 cm.

Above, Figure 12, a sample of three profile sections extracted on the integrated point clouds, aerial and ZEB scan (Figure 11), in which their different contribution to the geometry definition is pinpointed. It is important to point out, thanks to this section typology, the relevant contribution of the ZEB1 scans for the comprehensive definition of the building geometry. Below, alignment errors that are identified in Table 2 and are visible in a comparison map in range color on the sample in Figure 13, about the Building n°1. Statistical result of mean errors in clouds fitting results are very influenced first of all by the noise of the ZEB point clouds, and on the other hand, by the different accuracy reached by the aerial point cloud triangulation about the geometric definition in narrow spaces on ground. Excluding this point cloud noise and considering the significant areas of the buildings, the errors values in the comparisons below by clouds fitting algorithm

can be reasonably and limited under 10-15 cm, which satisfy the expected accuracy of the technological solution aims of rapid mapping and damage documentation.
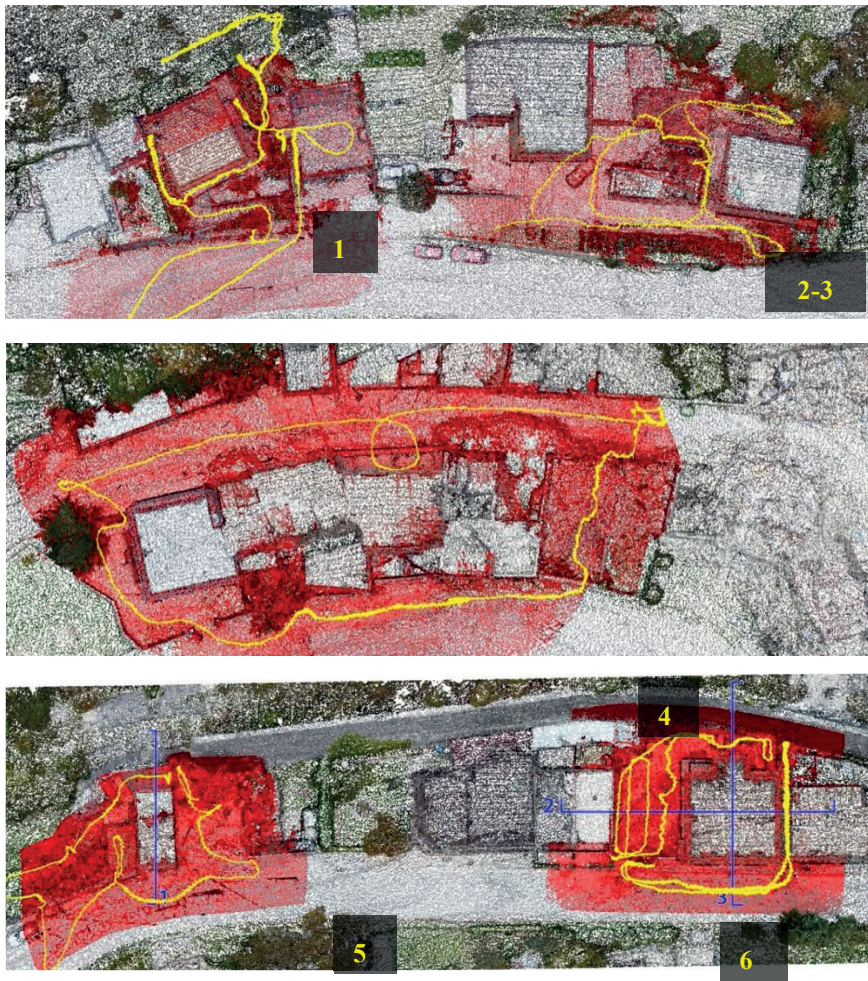

Figure 11. The aerial RGB point clouds and the ZEB1 georeferenced scans (red) with indicated the trajectory of acquisition (yellow), in order South, Center, North. Marked in blue, the sections profiles showed of Figure 12. The walkway and the path closure mode (Tracked trajectory in a closed ring or in a roundtrip through to the same path), influenced Simultaneous Localization And Mapping (SLAM) registration of the ZEB1 clouds, as visible here and in Table 2.
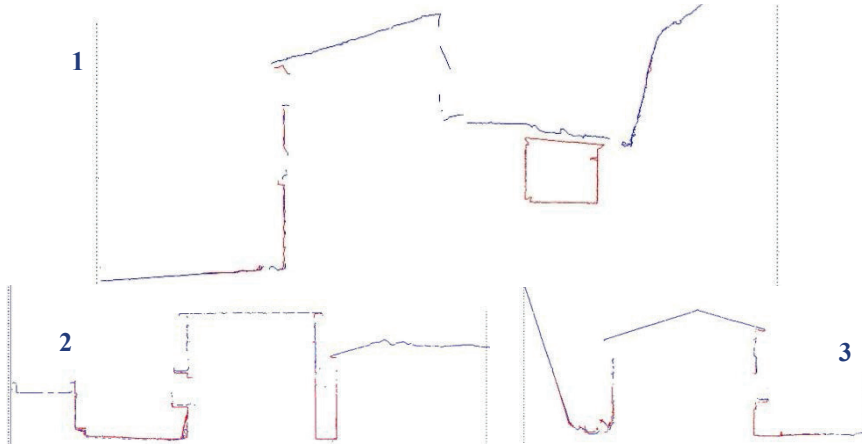
Figure 12. Three section profiles on northern block regarding the integration of point clouds. In blue colour the aerial contribution and in red the ZEB1 scan contribution.
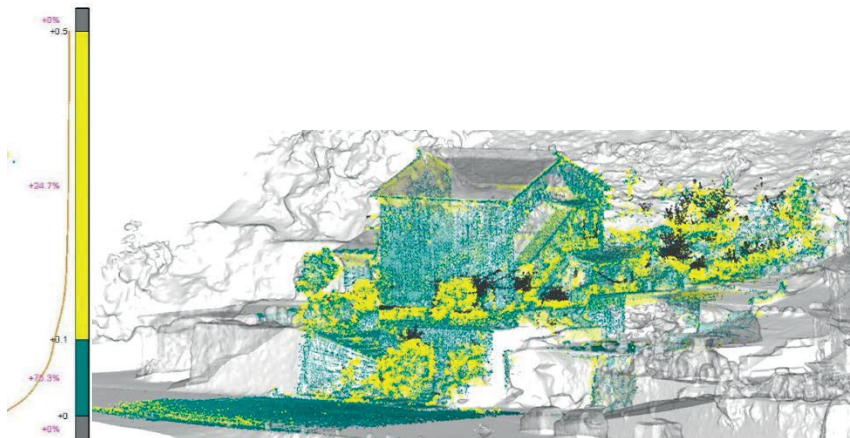

Figure 13. An example of cloud comparison, between ZEB and aerial photogrammetric one. Points statistically differ by 0.00 < **74.5%** < 0.10m (green)/0.01 < **24.7%** < 0.6m (yellow) (Details available in Table 1).

Table 2. Synthesis table of data processing results for the ZEB point clouds (Density values are expressed by n° of points in a spherical volume, with r = 1 cm).

Area	Building	N° Points	Density (pt/V. Sphere r = 0.01m)	Density St.dev	Alignment Mean Error (m)		
					0.00 < x < 0.10	0.10 < x < 0.30	0.03 < x < 0.60
South	B1	8.210.000	4.44	5.03	74.5%	20.8%	4.7%
	B2-3	14.500.000	3.35	3.80	68.4%	27.3%	4.2%
Center	B4	16.100.00	2.26	2.09	44.2%	50.2%	5,6%
North	B5	9.600.000	3.33	4.94	81.8%	12.5%	5.7%
	B6 (a+b)	15.800.000	3.73	3.90	69.4%	28.1%	2.4%

4. Deriving Metric and Non-Metric Data from 3D Model: A Test-Case

Starting from the subsequent reconnaissance missions in the area, the different datasets have been organized and combined, in order to evaluate and classify the level of detail and usability of the different data, and for which applicative context. The preliminary data processing of the Northern dataset was limited to a selected focus object: this building (n°5, Figure 11) is one of the been kept under the observation of the structural team.

A pertinence area around the test building have been chosen too (Figure 14). A large amount of information have been extracted from aerial and terrestrial acquisition and classified from images and 2D/3D production, as in following examples.

Figure 14. An images of the building n°5 in October 2016 and relative orthoimage by multi-rotor drone (aerial images of both shooting and frames extraction from 4k video with DJI drone).

4.1. Data Acquisition and Processing

Different datasets are trying to be integrated in the test area. In Figure 15, the datasets are listed: the aerial acquisition (distinguished by camera configuration),

and the photogrammetric model that is produced with both the camera configurations; the terrestrial close-range acquisition, and the fusion model using the complete dataset.

As it is said before, the topographic and GNSS survey were affected by site conditions and constraints, and the difficulties of freely positioning markers for measurements, together with GNSS signal problems from permanent stations. Here, the processed datasets referred to the Building n°5. Estimated errors on CP for each processing by RMSE analysis (table and graph in Figure 15) allow for us to choose the last one, the data fusion, as the ground-truth for further analysis. According to the information extraction strategy, 3D data must be processed for filtering by noise reduction and optimized to finalize a 3D model or 3D information as in next paragraphs.
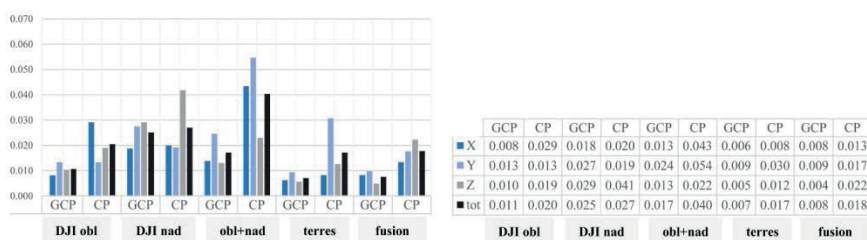

	GCP	CP	GCP	CP	GCP	CP	GCP	CP	GCP	CP
X	0.008	0.029	0.018	0.020	0.013	0.043	0.006	0.008	0.008	0.013
Y	0.013	0.013	0.027	0.019	0.024	0.054	0.009	0.030	0.009	0.017
Z	0.010	0.019	0.029	0.041	0.013	0.022	0.005	0.012	0.004	0.022
tot	0.011	0.020	0.025	0.027	0.017	0.040	0.007	0.017	0.008	0.018
	DJI obl		DJI nad		obl+nad		terres		fusion	

Figure 15. Accuracy on ground control points (GCPs) and Check Points (CPs) RMSE (m): DJI flights, fusion of aerial data, close-range acquisition, and global integration of photogrammetric datasets. We can consider this last one as the best verified result so that it can be used as ground-truth.

4.2. Evaluation on Multi-Sensor Data Acquisition and Information Interpretation, Classification and Extraction

Operating camera configuration and sensor integration, it is possible to make the 3D model accessible to different needs, and expertise information that is embedded in 3D data had not to be simply geometric. As we affirmed before, the great part of first building damage assessment (BDA) is still based on visual evaluation, and then the metric assessment of the metric structural condition of buildings, finalized to accessibility constraint.

4.2.1. Orthoimages and DSM

A photogrammetric model by commercial DJI drone, as in Orthoimage, is highly competitive in terms of quality of RGB information. The standard of comparison is a well-known terrestrial close-range photogrammetry, a solution that is less viable in these contexts of timing and accessibility to spaces. Most damages and creeps on all of the façades are clearly visible even in the aerial model (as in example in Figure 17), better than in the fusion one. More reflections

that are interesting to be carried out are on the typical aerial representation of the site surface. For a DSM, data extraction could usually concern, for example, isolines and elevation points. For the 3D documentation of the building and its surrounding areas at environmental scale, ZEB1 point cloud has provided good results, as in Figure 16. For planimetric information at architectonical scale, a HQ fusion model offers the best level of detail of the building and around (Figure 12).

Figure 16a. Comparison, on a small area, between used platforms and sensors: eBee, average GSD of 5 cm/pixel (left); DJI Phantom, average GSD of 2.18 cm/pixel (center left); fusion model, average GSD of 0.92 cm/pixel (center right); no RGB data from Zeb1.

(**a**)   (**b**)
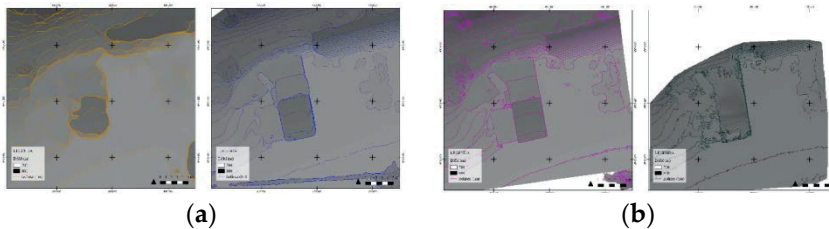
Figure 16b. DSM comparison. eBee (left); DJI (center right). Fusion model (center left); ZEB1 (right).

Figure 17. Orthoimage of the East side. The aerial model by integrated oblique and nadir cameras (right), can be comparable in terms of available detail and the accessible information to the terrestrial photogrammetric one (left).

4.2.2. Geometric Detail and Section Profiles

We identify some crucial points in the structure in which it could be very useful for a structural reconnaissance after a damage event. The main geometrical and structural building condition could be evaluated first of all with a series of horizontal and vertical sections that could better clarify any geometrical behavior of the volume, the façade, the roof, and the other main walls. Here, the transversal section, intersecting the point of weakness of the chimney axe, could show possible misalignments and out of plumb of the lateral masonries; in longitudinal section (Figure 18, Table 3) it is possible to analyse the openings and possible damages of the façade.
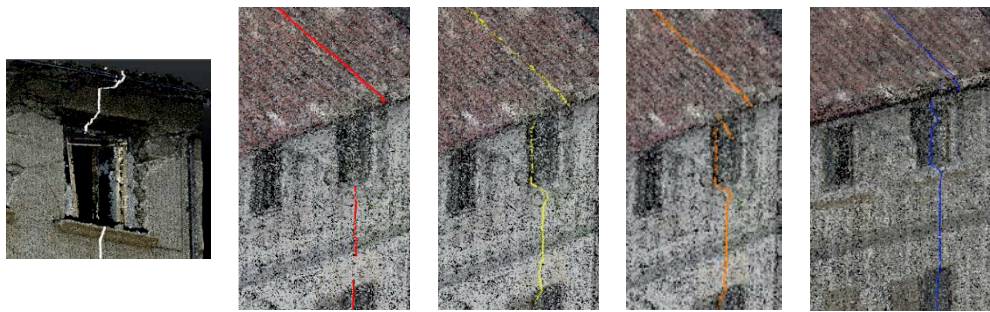
Figure 18. A zoomed portion of the longitudinal section superimposed to the fusion model showing the contribution to the geometric definition. From left: terrestrial photogrammetric model (white); nadir cameras (red); oblique cameras (yellow), aerial acquisitions model (orange), HQ data fusion model (blue).

Density indexes (Table 3) are here significantly for differentiate the contribution of each sensor for the geometrical definition. Despite the close-range one is the richer in dense points on the façade, is the most non-uniform (St. Dev), together with the ZEB1 one. As expected, the fusion model presents a uniform distribution of measurements of the whole building in comparison to the aerial one. We can verify that the fusion of models contributes to the geometric definition, not in terms of average density, but for the standardization of distribution.

We can affirm that the extensiveness data from fusion of terrestrial and aerial images can be integrated with a union of the LiDAR ZEB1 data (Figure 19) that have been georeferenced, in order to produce a complete profile of the building with hits geometry in relationship with the rear rock face.
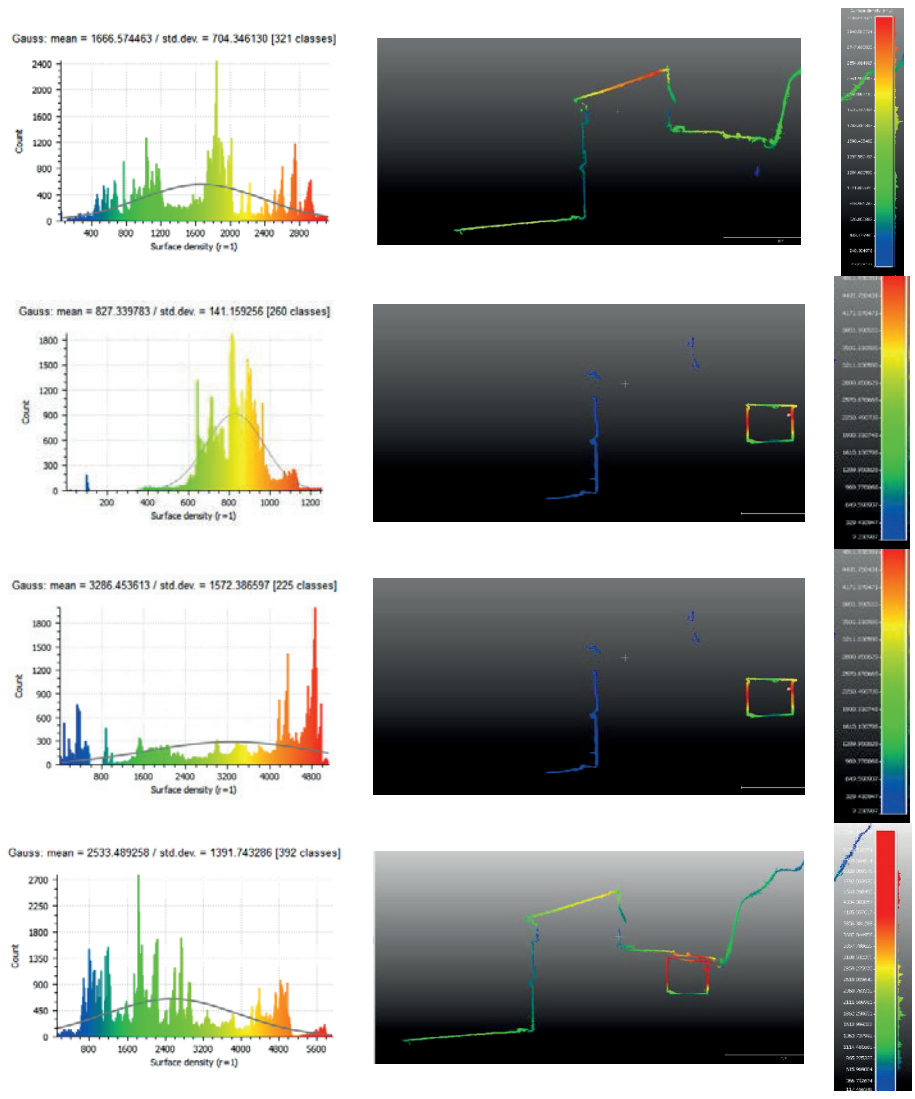
Figure 19. Density for aerial point cloud (1), data fusion point cloud (2), ZEB point cloud (3), and integrated Light Detection and Ranging (LiDAR) and aerial point cloud (4).

Table 3. Synthesis table of statistical values on longitudinal section (20 cm thickness).

			Longitudinal Section			
				Density (n° points)		
			n° points	Average Density (point/m²)	st.dev.	Min	Max
	ZEB		50,444	**3,286**	1,572	9	5100
	NIKON	high	370,716	**27,300**	7,200	84	37,220
	EBEE		806	12	3	1.9	18
	DJI	obl	95,119	1,578	658	1	2,970
		nad	8,667	128	35	16	197
		fusion	102,493	**1,666**	**704**	47	3,100
	FUSION	low	1,400	18	4	0.6	32
		med	12,111	147	31	0.9	228
		high	67,400	**827**	**141**	1	1,256
INTEGRATION AERIAL+ZEB POINTS CLOUD			152,937	**2,533**	1,392	117	5,936

5. Conclusions and Future Perspectives

In this contribution, a work-in-progress test approach for rapid mapping is presented, which is finalized to testing and refine the methodological approach, as well as improve the operational procedure with a view to a standardization, in the Geomatics techniques scenario, focused on rapid mapping in emergency contexts. A step-by-step analysis about procedures to acquire 3D data for rapid mapping by quick terrestrial scanning (ZEB1 portable scan) and aerial photogrammetry by COTS UAV equipment and sensors have been displayed. For an environmental scale in Pescara del Tronto, different areas according to blocks geometry and topographical conformation have been chosen and modelled with the contribution of aerial and terrestrial point clouds, and they give interesting results in terms of application according to the typological and topographical geometry of the object, as well as the surrounding. Therefore, it is also interesting to analyse the better practice of SLAM-based point clouds manipulation on outdoor environments (despite the implementation of this technique to be employed in indoor scenarios or otherwise in narrow locations). The aims of the proposed documentation approach is first of all the optimization of points clouds processing from a multi-sensor acquisition at different scale, in order to balance competitiveness of resources (human and technical) and the effectiveness of metric and non-metric information.

Afterward, in order to exploit the richness of metric and radiometric information of the 3D model optimization, a test building in a higher scale has been deepened. In this case, we can reflect that a high-quality model integration of models is preferable instead of a data fusion processing: extreme density on radiometric and metric information by close-range photogrammetry can be fulfil

165

by oblique image processing for upper parts. An indoor mapping, if practicable, can complete the reconnaissance multi-sensor model. In terms of accuracy, the realized model by data fusion finally has the lower discrepancy on CPs and better fits with the terrestrial measurements (Figure 15). Unless very accurate information is necessary for specific focus analysis on the building, an aerial model could be suitable; the integration of aerial and terrestrial does not add a significant improvement in level of geometric definition for a first-step damage documentation and assessment (Figure 14), and in any case, the detail of terrestrial imaging could not be reached. Nevertheless, according to the achieved results and preliminary analysis, is possible to underline that a UAV nadir-oblique close-range acquisition, open to improvement in the use of high resolution cameras, could obtain a very strategic level of information. It is not so much the density that rises using the aerial camera merging, but, of course, is the homogeneousness (st. dev values variation) cloud density, which allows for extracting less fractionated sections (Figure 18).

References

1. Aicardi, I.; Chiabrando, F.; Grasso, N.; Lingua, A.M.; Noardo, F.; Spanò, A. UAV photogrammetry with oblique images: First analysis on data acquisition and processing. *Int. Arch. Photogramm. Remote Sens. Spat. Inf. Sci.* **2016**, *XLI-B1*, 835–842.
2. Boccardo, P.; Chiabrando, F.; Dutto, F.; Tonolo, F.G.; Lingua, A. UAV Deployment Exercise for Mapping Purposes: Evaluation of Emergency Response Applications. *Sensors* **2015**, *15*, 15717–15737.
3. Bosse, M.; Zlot, R. Continuous 3D Scan Matching with a Spinning 2D Laser. In Proceedings of the 2009 ICRA'09 IEEE International Conference on Robotics and Automation, Kobe, Japan, 12–17 May 2009; pp. 4244–4251.
4. Bosse, M.; Zlot, R.; Flick, P. Zebedee: Design of a Spring-Mounted 3D Range Sensor with Application to Mobile Mapping. *IEEE Trans. Robot.* **2012**, *28*, 1104–1119.

5. Chiabrando, F.; Sammartano, G.; Spanò, A. A comparison among different optimization levels in 3D multi-sensor models. A test case in emergency context: 2016 Italian earthquake. *Int. Arch. Photogramm. Remote Sens. Spat. Inf. Sci.* **2017**, *XLII-2/W3*, 155–162.

6. Chiabrando, F.; D'Andria, F.; Sammartano, G.; Spanò, A. 3D Modelling from UAV Data in Hierapolis of Phrygia (TK). In Proceedings of the 8th International Congress on Archaeology, Computer Graphics, Cultural Heritage and Innovation 'ARQUEOLÓGICA 2.0', Valencia, Spain, 5–7 September 2016; pp. 347–349.

7. Chiabrando, F.; Di Pietra, V.; Lingua, A.; Maschio, P.; Noardo, F.; Sammartano, G.; Spanò, A. TLS models generation assisted by UAV survey. *Int. Arch. Photogramm. Remote. Sens. Spat. Inf. Sci.* **2016**, *XLI-B5*, 413–420.

8. Fernandez Galarreta, J.; Kerle, N.; Gerke, M. UAV-based urban structural damage assessment using object-based image analysis and semantic reasoning. *Nat. Hazards Earth Syst. Sci.* **2015**, *15*, 1087–1101.

9. Gerke, M.; Kerle, N. Automatic structural seismic damage assessment with airborne oblique Pictometry© imagery. *Photogramm. Eng. Remote Sens.* **2011**, *77*, 885–898.

10. Kerle, N. Satellite-based damage mapping following the 2006 Indonesia earthquake—How accurate was it? *Int. J. Appl. Earth Obs. Geoinf.* **2010**, *12*, 466–476, doi:10.1016/j.jag.2010.07.004.

11. Lemoine, G.; Corbane, C.; Louvrier, C.; Kauffmann, M. Intercomparison and validation of building damage assessments based on post-Haiti2010-earthquake imagery using multi-source reference data. *Nat. Hazards Earth Syst. Sci. Discuss.* **2013**, *1*, 1445–1486.

12. Lerma, J.L.; Seguí, A.E.; Cabrelles, M.; Haddad, N.; Navarro, S.; Akasheh, T. Integration of Laser Scanning and Imagery for Photorealistic 3D Architectural Documentation. In *Laser Scanning, Theory and Applications*; Wang, C.-C., Ed.; InTech Open: Rijeka, Croatia, 2011; doi:10.5772/14534.

13. Maier, P. Assessing Disaster Damage: How Close Do You Need to Be? 2016. Available online: https://irevolutions.org/2016/02/09/how-close/ (accessed on 28 July 2017).

14. Rathje, E.M.; Franke, K. Remote sensing for geotechnical earthquake reconnaissance. *Soil Dyn. Earthq. Eng.* **2016**, *91*, 304–316.

15. Rastiveis, H.; Samadzadegan, F.; Reinartz, P. A fuzzy decision making system for building damage map creation using high resolution satellite imagery. *Nat. Hazards Earth Syst. Sci.* **2013**, *13*, 455–472, doi:10.5194/nhess-13-455-2013.

16. Bosse, M.; Zlot, R.; Flick, P. Zebedee: Design of a Spring-Mounted 3D Range Sensor with Application to Mobile Mapping. *IEEE Trans. Robot.* **2012**, *28*, 1104–1119.

17. Remondino, F.; Barazzetti, L.; Nex, F.; Scaioni, M.; Sarazzi, D. UAV photogrammetry for mapping and 3D modeling–current status and future perspectives. *Int. Arch. Photogramm. Remote Sens. Spat. Inf. Sci.* **2011**, *38*, C22, doi:10.5194/isprsarchives-XXXVIII-1-C22-25-2011.

18. Riisgaard, S.; Blas, M. Slam for Dummies. A Tutorial Approach to Simultaneous Localization and Mapping, 2005. Available online: http://ocw.mit.edu/NR/rdonlyres/ Aeronautics-and-Astronautics (accessed on 28 July 2017).

19. Ruiz Sabina, J.; Gallego Valle, D.; Peña Ruiz, C.; Molero García, J.; Gómez Laguna, A. 2015. Aerial Photogrammetry by drone in archaeological sites with large structures. *Virtual Archaeol. Rev.* **2015**, *6*, 5–19, doi:10.4995/var.2015.4366.

20. Strecha, C. The rayCloud—A Vision Beyond the Point Cloud. In Proceedings of the FIG Congress 2014, Engaging the Challenges—Enhancing the Relevance, Kuala Lumpur, Malaysia, 16–21 June 2014.

21. Thomson, C.; Apostolopoulos, G.; Backes, D.; Boehm, J. Mobile laser scanning for indoor modelling. *Int. Arch. Photogramm. Remote. Sens. Spat. Inf. Sci.* **2013**, *II-5/W2*, doi:10.5194/isprsannals-II-5-W2-289-2013.

22. Voigt, S.; Scheneiderhan, T.; Twele, A.; Gahler, M.; Stein, E.; Mehl, H. Rapid damage assessment and situation mapping: Learning from the 2010 Haiti earthquake, *Photogramm. Eng. Remote Sens.* **2011**, *77*, 923–931.